DOI: 10.1002/ange.200904958

Iodinated Nanoscale Coordination Polymers as Potential Contrast Agents for Computed Tomography**

*Kathryn E. deKrafft, Zhigang Xie, Guohua Cao, Sylvie Tran, Liqing Ma, Otto Z. Zhou, and Wenbin Lin**

Computed tomography (CT) is a powerful diagnostic tool based on X-ray attenuation by a specimen, and is capable of providing three-dimensional (3D) images with excellent spatial resolution.[1] A contrast agent with high X-ray attenuation, typically materials containing elements with a high Z number such as iodine, barium, and bismuth, is often used in CT imaging to provide better contrast between the tissue of interest and its surroundings.[2] The only CT contrast agents currently approved for clinical use are iodinated aromatic molecules, and barium sulfate for gastrointestinal tract imaging. CT imaging with small-molecule contrast agents is limited by their nonspecific distribution, rapid renal clearance, and rapid extravasation from blood and lymphatic vessels.[2] Large doses of small-molecule agents (tens of grams) are typically needed to provide adequate contrast, which sometimes cause adverse reactions for the patients.

These limitations can be overcome by nanoparticulate contrast agents that can carry a high payload and be functionalized to increase blood circulation times and to endow target specificity.[3] Nanoparticles do not readily diffuse into extravascular space or undergo rapid renal clearance, thus allowing adequate time for accumulation at a disease site. These advantages could allow for a larger time window for imaging and enhanced image contrast at a lower dose. Several nanoparticle systems including Bi_2S_3,[4] gold,[5] and iodinated organic nanoparticles,[6] have recently been evaluated as next-generation CT contrast agents. However, it is challenging to formulate nanoparticles with high loadings for elements having high Z numbers that are also nontoxic and able to be cleared from the body in a timely fashion.

Coordination polymers have recently emerged as interesting functional materials that are readily synthesized by coordination-directed self-assembly of metal ions and organic bridging ligands.[7] Our research group and others have recently demonstrated the synthesis of a new class of nanomaterials by scaling down coordination polymers to the nano-regime.[8] These nanoscale coordination polymers (NCPs) have already shown great potential in biosensing,[9] magnetic resonance imaging,[10] and drug delivery.[11] Given the clinical utility of iodinated aromatic molecules in CT imaging, we surmised that iodinated NCPs could have potential applications as CT contrast agents owing to their ability to carry a very high payload of iodine. Herein we report the synthesis of new iodinated coordination polymers and their scale down to the nano-regime. We also demonstrate the ability of iodinated NCPs to attenuate X-rays in phantom studies.

As shown in Scheme 1, five new coordination polymers were synthesized using 2,3,5,6-tetraiodo-1,4-benzenedicarboxylic acid (I_4-BDC-H_2) bridging ligands and Cu^{II} or Zn^{II} metal connecting points. The reaction of I_4-BDC-H_2 and $Cu(NO_3)_2$ in *N*,*N*-dimethylformamide (dmf) at 80 °C for 3 days led to blue rectangular platelike crystals of $[Cu(I_4\text{-BDC})(dmf)_2]$ (**1**) in 28 % yield. Similar crystal growth in *N*,*N*-diethylformamide (def) and in H_2O led to bluish-green rodlike crystals of $[Cu(I_4\text{-BDC})(def)_2(H_2O)]$ (**2**) in 58 % yield and green rodlike crystals of $[Cu(I_4\text{-BDC})(H_2O)_2]\cdot 2H_2O$ (**3**) in 69 % yield, respectively. To demonstrate the generality of this synthetic approach, we have also synthesized iodinated coordination polymers with Zn^{II} metal connecting points. Colorless rodlike crystals of $[Zn(I_4\text{-BDC})(dmf)_{2.5}]$ (**4**) were obtained in 55 % yield by the reaction of I_4-BDC-H_2 and $Zn(NO_3)_2$ in dmf at 60 °C for 4 days. Colorless rodlike crystals of $[Zn(I_4\text{-BDC})(EtOH)_2]\cdot 2EtOH$ (**5**) were obtained in 28 %

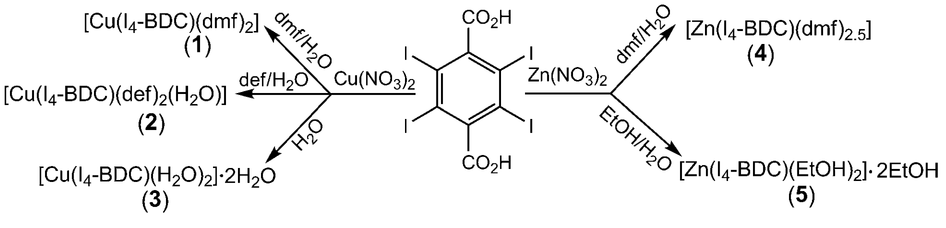

Scheme 1. Synthesis of five new coordination polymers.

---

[*] K. E. deKrafft, Dr. Z. Xie, S. Tran, Dr. L. Ma, Prof. W. Lin
Department of Chemistry, CB 3290, University of North Carolina
Chapel Hill, NC 27599 (USA)
Fax: (+1) 919-962-2388
E-mail: wlin@unc.edu
Homepage: http://www.chem.unc.edu/people/faculty/linw/wlindex.html
Dr. G. Cao, Prof. O. Z. Zhou
Department of Physics and Astronomy, University of North Carolina
Chapel Hill, NC 27599 (USA)

[**] We acknowledge financial support from the NIH (U54-CA119343) and the NSF (DMR-0906662).

Supporting information for this article is available on the WWW under http://dx.doi.org/10.1002/anie.200904958.

yield by slow evaporation of a solution of I_4-BDC-H_2 and $Zn(NO_3)_2$ in ethanol. The synthesis of coordination polymers in H_2O and in ethanol (**3** and **5**) demonstrates the ability to obtain iodinated coordination polymers that contain nontoxic solvents, thus making them more relevant for potential biological and biomedical applications.

Single-crystal X-ray diffraction studies of **1**–**5** revealed one-dimensional (1D) polymeric structures for all five coordination polymers (Figure 1).[12] In compound **1**, Cu^{II} ions coordinate to two chelating carboxylate groups of the I_4-BDC ligand and two molecules of dmf in the axial positions to form a 1D polymeric network (Figure 1 a). In compound **2**, both carboxylate groups of the I_4-BDC ligand are monodentate (Figure 1 b). The Cu^{II} ions adopt a square pyramidal geometry by coordinating to two monodentate carboxylate groups as well as one water and two def molecules. The structure of **3** is ladderlike with one carboxylate group of the ligand acting in a monodentate fashion, while the other adopts the η^1,μ_2 bridging mode (Figure 1 c). Each Cu^{II} center thus coordinates to three carboxylate oxygen atoms and two water molecules in a square pyramidal geometry. The distance between the adjacent I_4-BDC ligands in the 1D polymer is 4.06 Å. In compound **4**, one I_4-BDC ligand has both monodentate carboxylate groups whereas the other I_4-BDC ligand has one monodentate and one chelating carboxylate group (Figure 1 d). The adjacent Zn^{II} centers in the zigzag polymeric chain adopt a tetrahedral geometry by coordinating to two monodentate carboxylate groups and two def molecules, and a distorted octahedral geometry by coordinating to one monodentate and one chelating carboxylate groups and three def molecules, respectively. Compound **5** has a simpler zigzag polymeric chain structure with all the Zn^{II} centers adopting tetrahedral geometry by coordinating to two monodentate carboxylate groups and two ethanol molecules (Figure 1 e). Importantly, the steric bulk of the iodine atoms forces the carboxylate groups of the I_4-BDC ligand to be perpendicular to the tetraiodobenzene ring in all of these structures. We believe that the steric bulk of iodine atoms also discourages the carboxylate groups of the I_4-BDC ligands from adopting the bridging coordination mode (except in **3**), which can lead to the formation of coordination polymers of higher dimensionality. The thermogravimetric analyses (TGA) of bulk crystals of **1**–**5** show solvent and organic weight loss that corresponds closely to the formulas obtained from X-ray diffraction data (see the Supporting Information).

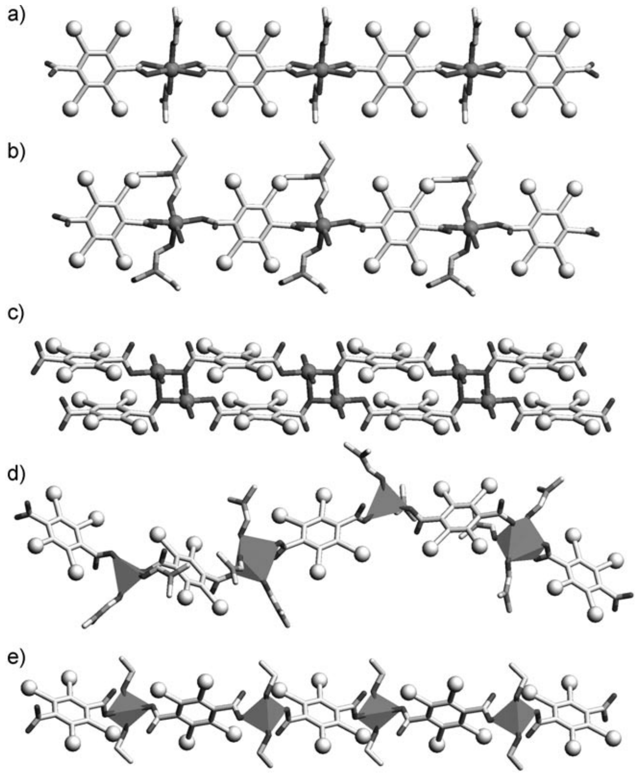

Figure 1. Single-crystal X-ray structures of 1D coordination polymers of a) $[Cu(I_4\text{-BDC})(dmf)_2]$ (**1**), b) $[Cu(I_4\text{-BDC})(def)_2(H_2O)]$ (**2**), c) $[Cu(I_4\text{-BDC})(H_2O)_2]\cdot 2H_2O$ (**3**), d) $[Zn(I_4\text{-BDC})(dmf)_{2.5}]$ (**4**), and e) $[Zn(I_4\text{-BDC})(EtOH)_2]\cdot 2EtOH$ (**5**). Stick joints: C (light gray), N (medium gray), O (dark gray); balls: I (light gray), Cu (dark gray). Coordination around Zn atoms (d,e) are shown as gray polyhedra.

We were able to synthesize nanoparticles of both a Cu^{II}- and a Zn^{II}-containing phase, with coordinating H_2O and ethanol molecules, respectively. Platelike nanoparticles of **3** (NCP **3a**) were synthesized in 75% yield by stirring a microemulsion of 0.3 M Triton X-100 and 1.5 M 1-hexanol in with a water to surfactant ratio of 15 (*W* value), which contained equal molar amounts of $Na_2(I_4\text{-BDC})$ and $Cu(NO_3)_2$ at room temperature for 2 h. The NCP **3a** particles were isolated by centrifugation and washed with ethanol. Scanning electron microscopy (SEM) images showed that platelike particles of NCP **3a** have a diameter of 300 nm and are 50 nm thick (Figure 2 a). Powder X-ray diffraction (PXRD) studies indicate that the NCP **3a** particles are crystalline and have the same structure as the bulk phase of **3** (Figure 2 c). Interestingly, nanoparticles of **3** with a rodlike

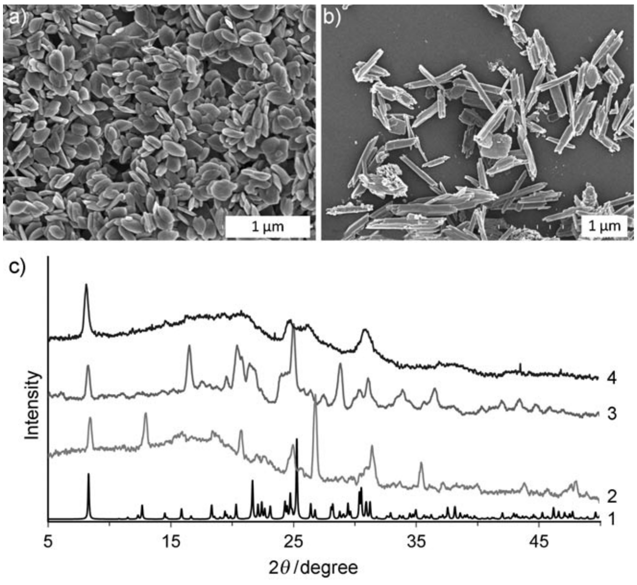

Figure 2. a) SEM images of NCP **3a** and b) NCP **3b**. c) Simulated PXRD pattern of **3** (1), and experimental PXRD patterns of bulk crystals of **3** (2), NCP **3a** (3), and NCP **3b** (4).

morphology (NCP **3b**) were obtained in 60% yield when the same reaction was carried out in a microemulsion of 0.1 M cetyltrimethylammonium bromide and 0.5 M 1-hexanol in isooctane ($W=15$). SEM images show that NCP **3b** particles are about 1.5 µm in length and 200 nm in width (Figure 2b), and PXRD studies indicate that the particles are crystalline and also have the same structure as the bulk phase of **3**. The composition of NCP **3a** and NCP **3b** was also confirmed by TGA and energy dispersive X-ray spectroscopy (EDS) results. Slight peak shifts in the PXRD patterns can be attributed to differences in the temperatures at which data were acquired and the degree of solvent loss from the sample, both of which can slightly change the size of the unit cell. Many of the diffraction peaks are missing in the PXRD patterns of the NCPs because of the preferential growth along certain crystallographic faces.

We synthesized microparticles of **5** using a rapid precipitation procedure.[11] A dilute aqueous solution of $Na_2(I_4\text{-}BDC)$ and $Zn(NO_3)_2$ in an equal molar ratio was added to ethanol with rapid stirring. SEM and PXRD studies showed that the resulting particles (NCP **5a**) were crystalline rods having a less than µm width and were 10–30 µm in length (Figures 3a,c). We found that smaller particles NCP **5b** could be obtained by addition of a more concentrated aqueous precursor solution (pH 6.6) to ethanol. The resulting white cloudy dispersion was stirred at room temperature for 1 hour. The NCP **5b** nanoparticles were isolated in 82% yield by centrifugation and washed with ethanol. SEM images show that the NCP **5b** particles have a truncated cube morphology with a diameter of 200–600 nm (Figure 3b). PXRD studies show that they match the bulk phase of **5** (Figure 3c), but the very broad peak indicates a large degree of disorder in the structure of these partially crystalline particles. The composition of NCP **5a** and NCP **5b** was also confirmed by TGA and EDS results.

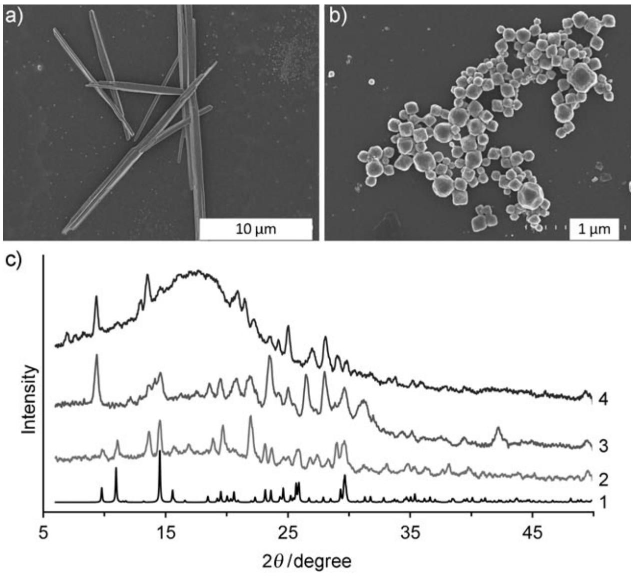

Figure 3. a) SEM images of NCP **5a** and b) NCP **5b**. c) Simulated PXRD pattern of **5** (1), and experimental PXRD patterns of bulk crystals of **5** (2), NCP **5a** (3), and NCP **5b** (4).

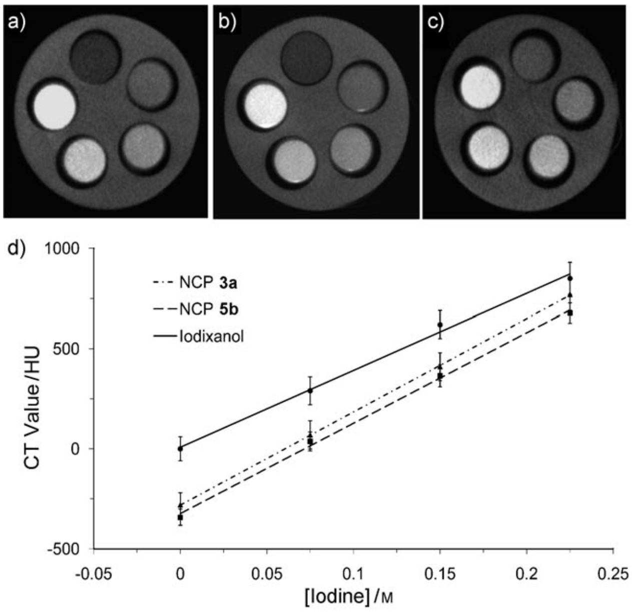

Figure 4. CT phantom images of a) NCP **3a** and b) NCP **5b** dispersed in ethanol, and c) Iodixanol in aqueous solution. From the top, clockwise, the slots have [I] = 0, 0.075, 0.150, 0.225, and 0.300 M. d) X-ray attenuation as a function of [I] for NCP **3a** at 40 kVp, NCP **5b** at 50 kVp, and Iodixanol at 40 kVp.

We conducted phantom studies on NCP **3a** and NCP **5b** to evaluate their potential for use as CT contrast agents. Scans were done on ethanol dispersions with corresponding iodine concentrations of 0–0.3 M (Figures 4a,b).[13] For comparison, samples of aqueous solutions of Iodixanol, a clinically used iodinated contrast agent, were also scanned at the same iodine concentrations (Figure 4c). Both NCP **3a** and NCP **5b** contain 63 wt% of iodine, while Iodixanol contains only 49 wt% iodine.[14] The theoretical iodine payload is 63.2 and 55.3 wt% for NCP **3a** and NCP **5b**, respectively, based on the formulas determined by X-ray diffraction data. The higher than predicted iodine payload for NCP **5b** is due to ready loss of ethanol molecules from the nanoparticles as shown in the TGA. For comparison, a recently reported polymer-stabilized lipid nanoparticle contains only 19 wt% iodine in the core, and iodine loading is even lower when the polymer shell is taken into consideration.[6a] The Hounsfield unit (HU)[15] value is an indicator of the ability of a material to attenuate X-rays with respect to water (0 HU). The slopes of the lines produced by plotting HU values against iodine concentrations for NCP **3a**, NCP **5b**, and Iodixanol are (4653 ± 520), (4513 ± 408), and (3840 ± 560) HU/M, respectively (Figure 4d). The nanoparticles thus show X-ray attenuation coefficients comparable to that of the molecular contrast agent. The slightly higher X-ray attenuation of the NCPs can be attributed to the contribution from Cu and Zn, calculated to be approximately 5% based on the weight% of these metals in the materials and the attenuation of the metals compared to that of iodine.

The biodegradable nature of NCPs makes them attractive candidates for imaging applications, because it is important that a diagnostic agent be cleared from the body after use.[8a,10b] To determine the dissolution (degradation) behavior of the iodinated NCPs in a biologically relevant environment, we dialyzed NCP **3a** against phosphate buffered saline (PBS; pH 7.4) at 37 °C. The particles were completely dissolved after approximately 46 hours, with a half-life of about 1.5 hours (Figure S10 in the Supporting Information). This result demonstrates the biodegradable nature of the NCPs while they are still stable enough to allow for longer circulation time as compared to molecular iodinated contrast agents ($<$ 10 min).

In summary, we have synthesized novel iodinated coordination polymers as well as corresponding nanoparticle phases with controllable morphologies and demonstrated their potential for CT contrast enhancement. These new nanomaterials are capable of delivering high payloads of iodine and offer a new strategy for designing efficient CT contrast agents that do not suffer from the inherent drawbacks of small-molecule agents.

Experimental Section

A typical procedure for crystal growth: **1** was synthesized by dissolving I_4-BDC-H_2 (4.02 mg, 6.00 μmol) and $Cu(NO_3)_2{\cdot}3H_2O$ (1.45 mg, 6.00 μmol) in a mixture of dmf (670 μL) and H_2O (34 μL) with HCl (1 equiv, 6.00 μmol). The vial containing the resulting clear solution was capped and placed in an 80 °C oven. After 3 days blue, rectangular plate-shaped crystals were obtained in a yield of 1.46 mg (27.7 %).

Synthesis of NCP **3a**: Two microemulsions with $W = 15$ were prepared by the addition of 1.215 mL of an aqueous solution of I_4-BDC sodium salt (0.1 M, pH 9.6) and 1.215 mL of a 0.1 M $Cu(NO_3)_2$ aqueous solution to separate 15 mL aliquots of a 0.3 M Triton X-100 and 1.5 M 1-hexanolin cyclohexane. The separate microemulsions were stirred vigorously for 10 min at RT before the two microemulsions were combined, and the resultant 30 mL microemulsion with $W = 15$ was stirred for an additional 2 h at RT. The nanoparticles were isolated by centrifugation at 13 000 rpm for 10 min. After the removal of the supernatant the particles were washed twice using 10 mL of ethanol each time. For each wash, the particles were redispersed by sonication and then recovered by centrifugation at 13 000 rpm for 10 min to give a yield of 69.9 mg (75.0 %).

Synthesis of NCP **5b**: A 200 μL aqueous precursor solution of 0.05 M $Na_2(I_4$-BDC) and 0.05 M $Zn(NO_3)_2$ was prepared and its pH was adjusted to 6.6 with NaOH. This precursor solution was quickly transferred into 25 mL of ethanol in a 50 mL round bottom flask with rapid stirring. This resulted in the immediate formation of a white cloudy dispersion, which was stirred at RT for 1 h. The product was isolated and washed as described above for NCP **3a** to give a yield of 6.35 mg (81.5 %).

Received: September 3, 2009
Revised: October 25, 2009
Published online: November 24, 2009

Keywords: computed tomography · contrast agents · coordination polymers · iodine · nanoparticles

---

[1] a) E. Seeram, *Computed Tomography: Physical Principles, Clinical Application, and Quality Control*, 3rd ed., Saunders/Elsevier, St. Louis, **2009**; b) W. A. Kalender, *Phys. Med. Biol.* **2006**, *51*, R29.

[2] a) U. Speck in *Handbook of Experimental Pharmacology, Vol. 185* (Eds.: W. Semmler, M. Schwaiger), Springer, Berlin, **2008**, pp. 167–175; b) A. Rutten, M. Prokop, *Anti-Cancer Agents Med. Chem.* **2007**, *7*, 307–316; c) W. Krause, P. W. Schneider, *Top. Curr. Chem.* **2002**, *222*, 107–150; d) S. Yu, A. D. Watson, *Chem. Rev.* **1999**, *99*, 2353.

[3] N. Matsuura, J. A. Rowlands, *Med. Phys.* **2008**, *35*, 4474.

[4] O. Rabin, J. M. Perez, J. Grimm, G. Wojtkiewicz, R. Weissleder, *Nat. Mater.* **2006**, *5*, 118.

[5] a) D. Kim, S. Park, J. H. Lee, Y. Y. Jeong, S. Jon, *J. Am. Chem. Soc.* **2007**, *129*, 7661; b) V. Kattumuri, K. Katti, S. Bhaskaran, E. J. Boote, S. W. Casteel, G. M. Fent, D. J. Robertson, M. Chandrasekhar, R. Kannan, K. V. Katti, *Small* **2007**, *3*, 333.

[6] a) D. Pan, T. A. Williams, A. Senpan, J. S. Allen, M. J. Scott, P. J. Gaffney, S. A. Wickline, G. M. Lanza, *J. Am. Chem. Soc.* **2009**, *131*, 15522; b) F. Hyafil, J.-C. Cornily, J. E. Feig, R. Gordon, E. Vucic, V. Amirbekian, E. A. Fisher, V. Fuster, L. J. Feldman, Z. A. Fayad, *Nat. Med.* **2007**, *13*, 636; c) A. Galperin, D. Margel, J. Baniel, G. Dank, H. Biton, S. Margel, *Biomaterials* **2007**, *28*, 4461.

[7] a) O. M. Yaghi, M. O'Keeffe, N. W. Ockwig, H. K. Chae, M. Eddaoudi, J. Kim, *Nature* **2003**, *423*, 705; b) O. R. Evans, W. Lin, *Acc. Chem. Res.* **2002**, *35*, 511; c) C. Wu, A. Hu, L. Zhang, W. Lin, *J. Am. Chem. Soc.* **2005**, *127*, 8940; d) G. Ferey, C. Mellot-Draznieks, C. Serre, F. Millange, *Acc. Chem. Res.* **2005**, *38*, 217.

[8] a) W. Lin, W. J. Rieter, K. M. L. Taylor, *Angew. Chem.* **2009**, *121*, 660; *Angew. Chem. Int. Ed.* **2009**, *48*, 650; b) A. M. Spokoyny, D. Kim, A. Sumrein, C. A. Mirkin, *Chem. Soc. Rev.* **2009**, *38*, 1218.

[9] W. J. Rieter, K. M. L. Taylor, W. Lin, *J. Am. Chem. Soc.* **2007**, *129*, 9852.

[10] a) W. J. Rieter, K. M. L. Taylor, H. An, W. Lin, W. J. Lin, *J. Am. Chem. Soc.* **2006**, *128*, 9024; b) K. M. L. Taylor, W. J. Rieter, W. Lin, *J. Am. Chem. Soc.* **2008**, *130*, 14358.

[11] W. J. Rieter, K. M. Pott, K. M. L. Taylor, W. Lin, *J. Am. Chem. Soc.* **2008**, *130*, 11584.

[12] Single-crystal X-ray diffraction data were measured on a Bruker SMART Apex II CCD-based X-ray diffractometer system equipped with a Cu-target X-ray tube ($\lambda = 1.54178$ Å). Crystal data for **1**: Orthorhombic, space group: $CmcC2_1$, $a = 10.928(1)$, $b = 21.668(2)$, $c = 9.579(1)$ Å, $V = 2268.1(3)$ Å^3, $\rho_{calc} = 2.569$ g cm^{-3}. Crystal data for **2**: Monoclinic, space group: $P2_1$, $a = 11.175(1)$, $b = 10.114(1)$, $c = 12.246(1)$ Å, $\beta = 107.293(2)°$, $V = 1321.5(1)$ Å^3, $\rho_{calc} = 2.386$ g cm^{-3}. Crystal data for **3**: Monoclinic, space group: $P2_1/c$, $a = 11.020(1)$, $b = 9.690(1)$, $c = 15.937(1)$ Å, $\beta = 105.164(5)°$, $V = 1642.5(2)$ Å^3, $\rho_{calc} = 3.248$ g cm^{-3}. Crystal data for **4**: Orthorhombic, space group: $P2_12_12_1$, $a = 10.387(1)$, $b = 11.758(1)$, $c = 38.819(2)$ Å, $V = 4740.9(3)$ Å^3, $\rho_{calc} = 2.566$ g cm^{-3}. Crystal data for **5**: Monoclinic, space group: $C2/c$, $a = 11.433(1)$, $b = 14.879(1)$, $c = 15.438(1)$ Å, $\beta = 95.718(1)°$, $V = 2613.16(9)$ Å^3, $\rho_{calc} = 2.327$ g cm^{-3}. CCDC 744845, 745368, 744106, 744846, and 744107 contain the supplementary crystallographic data for this paper. These data can be obtained free of charge from The Cambridge Crystallographic Data Centre via www.ccdc.cam.ac.uk/data_request/cif.

[13] G. Cao, Y. Z. Lee, R. Peng, Z. Liu, R. Rajaram, X. Calderon-Colon, L. An, P. Wang, T. Phan, S. Sultana, D. S. Lalush, J. P. Lu, O. Zhou, *Phys. Med. Biol.* **2009**, *54*, 2323.

[14] The amount of iodine that can be incorporated in small-molecule agents is limited by the need for side chains that increase hydrophilicity and decrease osmolality, viscosity, and toxicity.

[15] R. A. Brooks, *J. Comput. Assist. Tomo.* **1977**, *1*, 487.